




## Article

# A Substrate–Product Switch Mathematical Model for the Growth Kinetics of Ethanol Metabolism from Longan Solid Waste Using *Candida tropicalis*

Juan Feng <sup>1,2</sup>, Chatchadaporn Mahakuntha <sup>1,2</sup>, Su Lwin Htike <sup>1,2</sup>, Charin Techapun <sup>1,2</sup> , Yuthana Phimolsiripol <sup>1,2</sup> , Pornchai Rachtanapun <sup>1,2</sup> , Julaluk Khemacheewakul <sup>1,2</sup> , Siraphat Taesuwan <sup>1,2,3</sup>, Kritsadaporn Porninta <sup>1,2,4</sup> , Sumeth Sommanee <sup>1,2</sup>, Rojarej Nunta <sup>1,5</sup> and Noppol Leksawasdi <sup>1,2,\*</sup> 

<sup>1</sup> Center of Excellence in Agro Bio-Circular-Green Industry (Agro BCG), Faculty of Agro-Industry, Chiang Mai University, Chiang Mai 50100, Thailand; juan\_f@cmu.ac.th (J.F.); chatcha143dp@gmail.com (C.M.); sulwinhtike.n@alumini.cmu.ac.th (S.L.H.); charin.t@cmu.ac.th (C.T.); yuthana.p@cmu.ac.th (Y.P.); pornchai.r@cmu.ac.th (P.R.); julaluk.kh@cmu.ac.th (J.K.); siraphat.t@cmu.ac.th (S.T.); kritsadaporn.p@cmu.ac.th (K.P.); sumeth.s@cmu.ac.th (S.S.); rojarej@g.lpru.ac.th (R.N.)

<sup>2</sup> Faculty of Agro-Industry, Chiang Mai University, Chiang Mai 50100, Thailand

<sup>3</sup> Functional Foods and Nutrition Research (FFNR) Laboratory, University of Canberra, Nggunnawal Country, Bruce, ACT 2617, Australia

<sup>4</sup> Multidisciplinary Research Institute, Chiang Mai University, Chiang Mai 50200, Thailand

<sup>5</sup> Division of Food Innovation and Business, Faculty of Agricultural Technology, Lampang Rajabhat University, Lampang 52100, Thailand

\* Correspondence: noppol.l@cmu.ac.th; Tel.: +66-819506544

## Abstract

A substrate–product switch model was proposed to describe ethanol fermentation from longan solid waste using *Candida tropicalis* at an initial glucose and xylose ratio of 2 to 1. The model incorporated multiple rate equations for cell growth, sugar uptake, and ethanol production along with ethanol consumption. It elucidated the following three-step mechanism: (I) sugar uptake, (II) sugar conversion, and (III) ethanol consumption concerning the effects of concentration factor (*CF*) and associated growth function. Optimal kinetic parameters were estimated and validated against experimental data. The identification of two critical xylose concentrations showed that ethanol consumption either preceded or coincided with xylose consumption cessation. The phenolics inhibitory effect of gallic acid, ellagic acid, pyrogallol, and catechol on cell growth and ethanol production was elucidated with relatively minimal effect. The highest ethanol concentration of 25.5 g/L was reached with corresponding ethanol mass yield and productivity of 0.30 g/g and 1.063 g/L/h, respectively. The proposed model and kinetics provide valuable insights for designing and optimizing ethanol fermentation, contributing to more sustainable and cost-effective ethanol production.

**Keywords:** longan solid waste; substrate–product switch model; *Candida tropicalis*; kinetic parameters; ethanol fermentation; sustainable process



Academic Editor: Dongyang Liu

Received: 13 May 2025

Revised: 6 July 2025

Accepted: 7 July 2025

Published: 9 July 2025

**Citation:** Feng, J.; Mahakuntha, C.; Htike, S.L.; Techapun, C.; Phimolsiripol, Y.; Rachtanapun, P.; Khemacheewakul, J.; Taesuwan, S.; Porninta, K.; Sommanee, S.; et al. A Substrate–Product Switch Mathematical Model for the Growth Kinetics of Ethanol Metabolism from Longan Solid Waste Using *Candida tropicalis*. *Agriculture* **2025**, *15*, 1472. <https://doi.org/10.3390/agriculture15141472>

**Copyright:** © 2025 by the authors.

Licensee MDPI, Basel, Switzerland.

This article is an open access article distributed under the terms and conditions of the Creative Commons Attribution (CC BY) license (<https://creativecommons.org/licenses/by/4.0/>).

## 1. Introduction

Ethanol is an alternative sustainable fuel with a yearly production of 27 billion gallons [1]. In comparison to the conventional fossil counterparts, higher-octane number and significant heat of vaporization are well recognized qualities of ethanol [2]. Ethanol adoption could decrease carbon emissions from fossil fuels by over 80% [3]. In order to

counteract greenhouse gas emissions and dependency on fossil fuels, ethanol was blended into gasoline at different ratios, for example, 10% ethanol (E10) and 85% ethanol (E85) in several countries.

Currently, ethanol production from lignocellulosic biomass has gained popularity due to the widespread availability and cost-effectiveness of the feedstock [3]. The agricultural waste such as corn cob [4], sugarcane bagasse [5], wheat straw [6], and rice straw [7] has been used for ethanol production. Longan solid waste (LSW), a residue left from the whole fruit after longan juice extraction, is a potential source of lignocellulosic biomass for ethanol production. It contains high starch and low lignin content, which can eliminate the need for chemical pretreatment and enhance the recovery of fermentable sugars [8–10]. However, like other lignocellulosic biomass feedstock, the hydrolysate obtained from LSW contains both pentose and hexose sugars. Investigations on fermentation system utilizing sugars mixture revealed the highest ethanol production at a glucose to xylose ratio of 2:1 [11]. This ratio is commonly tested, yielding ethanol at 0.45–0.5 g/g with an average productivity of 0.9 g/L/h [12].

To improve ethanol production from mixture sugars, the following four main strategies have been reported: (1) enhancing sugars utilization, particularly xylose, through strain engineering or co-culture or sequence culture systems; (2) optimizing the production process by adjusting environmental conditions; (3) scaling up fermentation using fed-batch or continuous system with tailored feeding strategies; and (4) refining ethanol recovery techniques [13–16]. However, most of the findings are based on the operational observations and experimental measurements, which may not fully elucidate the complex reactions occurring during the fermentation process. Considering the continuous large-scale production, certain challenges and knowledges gaps in the fermentation process should be better explored.

Modeling is an important tool for understanding the fermentation process, aiding in process control, and improving production efficiency. The modeling in ethanol fermentation helps describe and predict the behavior of microbial growth, substrates consumption, and ethanol production under various conditions. For instance, sugar consumption and ethanol production using *Saccharomyces cerevisiae*, *S. stipites* (ATCC 58784), and *S. stipites* (ATCC 58785) for the treatment of waste hydrolysate after the tea detoxification process were elucidated by the Baranyi and Weibull models, Morgan-Mercer-Flodin model, and Stannard model, respectively [17]. A hybrid unstructured and structured model simulated substrate consumption, biomass, carbon dioxide, and ethanol production from cocoa waste using *Pichia kudriavzevii* [18]. Once a model is defined, further analysis of the kinetic parameters can enhance the understanding of the fermentation dynamics, optimize process conditions, and improve ethanol yield [19,20].

Besides the yeast species of *S. cerevisiae* [21], *Zymomonas mobilis* [22], *P. stipites* [23], and *Candida tropicalis* [24] were widely used in industrial lignocellulosic ethanol production. *C. tropicalis* offers the advantages of utilizing both glucose and xylose and providing greater versatility in lignocellulosic ethanol production. Despite its potential, there is a lack of comprehensive studies analyzing its fermentation kinetics, particularly at a glucose and xylose ratio of 2:1. Understanding the behavior of *C. tropicalis* under these conditions through experimental and modeling approaches can provide valuable insights for process optimization and industrial-scale applications.

In this study, twelve batches of ethanol fermentations from LSW hydrolysate were performed with the total sugar concentration of 30–200 g/L at a glucose and xylose ratio of 2:1 using *C. tropicalis* TISTR 5306. The inhibitory effect of phenolics on yeast cells and ethanol production was discussed. The main objectives of this study were to develop an unstructured mathematical model that accurately represents the metabolic activities of

sugar uptake, cell growth, and ethanol production from glucose and xylose mixture using *C. tropicalis*. The concentration factor (CF) and associated growth function were included to reflect extracellular substrates availability and intracellular bioconversion metabolic activity. This is the first model that integrates key kinetic parameters to capture the dynamic shifts in substrate utilization and metabolic transitions. Compared to conventional empirical models, this approach provides deeper mechanistic insights into the fermentation process and enables improved predictive accuracy of process control and ethanol yield optimization.

## 2. Materials and Methods

### 2.1. Microorganism, Inoculum Preparation, and Cultivation

*C. tropicalis* TISTR 5306 was ordered from the yeast strain collection of the Thailand Institute of Scientific and Technological Research (TISTR), cultured, and maintained on Yeast-Malt (YM) agar as described previously [10]. Liquid inoculum in 100 mL aliquot was prepared freshly from a sub-cultured agar plate by transferring a single full inoculation loop to YM medium in a 250 mL Erlenmeyer flask. Sufficient batches of these inoculated flasks were prepared for an addition of 10% (*v/v*) inoculum size in Section 2.3. The agitation speed for microbial cultivation was set at 100 rpm using a temperature controlled orbital shaker (Dihan Labtech, Model LCI 3016A, Jakarta, Indonesia) at 30 °C for 24 h [25]. The quality of cell culture in terms of viable and total cells count was assessed based on the hemocytometer technique, as described elsewhere [10], with a cell viability of 90% or higher.

### 2.2. Longan Solid Waste Hydrolysate Preparation

Longan (*Dimocarpus longan* Lour.)—assorted grade—was purchased from longan orchards in District of Saraphi, Chiang Mai, Thailand. The whole fruit was milled using a hammer mill (Crompton Controls, Model series 2000, Wakefield, UK) and a 40-mesh size sieve. The main composition of the solid fraction of LSW was as follows (*w/w*): 22.4 cellulose, 20.4 hemicellulose, 5.79 lignin, 27.9 starch, and 2.07 pectin. The LSW hydrolysate was obtained by one-step enzymatic hydrolysis using commercial enzyme mixtures of amylase, glucoamylase, cellulase, and xylanase with enzyme loading or an enzyme solution-to-buffer-volume ratio of 1:10 (10% *v/v*) at 50 °C for 48 h [10,14]. The evaporation process was used to concentrate this hydrolysate to a total sugar concentration of 200 g/L using a rotary evaporator (Greatwall, Model No. R-1010, Henan, China) at 70 °C for the media preparation [25]. The concentrated LSW hydrolysate contained the following: 143 g/L of glucose, 66.3 g/L of xylose, 1006 mg/L of gallic acid, 690 mg/L of ellagic acid, 242 mg/L of pyrogallol, and 35.0 mg/L of catechol. The concentration ratio of glucose to xylose in the concentrated LSW hydrolysate was thus 2.16.

### 2.3. Ethanol Production from Longan Solid Waste Hydrolysate

Ethanol production from LSW hydrolysate was carried out in 2 L Erlenmeyer flasks with 1.6 L of working volume at 30 °C with an initial pH of 6.0 under microaerobic conditions. The concentrated LSW hydrolysate in Section 2.2 was diluted until the concentration factors (CF) of 1.0, 1.1, 1.2, 1.3, 1.4, 1.5, 1.6, 1.8, 2.0, 3.0, 5.0, and 7.0 were reached, respectively, where the CF of 1.0 contained initial glucose + xylose concentrations of 20.8 + 9.78 g/L (see Supplementary Material for complete LSW hydrolysate compositions at varying CF). The concentration ratios of glucose to xylose in all cases were from 2.1–2.2 to 1.0. Additional ammonium sulfate of 8.52 g/L was used as the main nitrogen source [26]. The CF groups of 1.0, 1.2, 1.4, 1.6, and 2.0 were used for optimal parameters searching. The model validation was performed with CF groups of 1.1, 1.3, 1.5, and 1.8 to evaluate the interpolative capability of the model. The extrapolative (3.0) and extended extrapolative (5.0 and 7.0) capability of the model were also assessed. Each experiment was performed in quintuplicate with regular

sampling every 6 h until the end of cultivation at 48 h. The concentrations determination of glucose, xylose, ethanol, dried biomass, gallic acid, ellagic acid, pyrogallol, and catechol were performed later, as described in Section 2.4.

#### 2.4. Analytical Techniques

Dried biomass concentration was determined using cell sediments from collected fermentation broth through a centrifugation process at  $2822 \times g$  (5000 rpm) for 10 min. A double cell-washing process with distilled water was implemented before drying at  $105^\circ\text{C}$  until constant weight was reached. Glucose, xylose, and ethanol concentrations were quantified by high performance liquid chromatography (HPLC, Agilent Technologies, Model No. HP1260, USA) using 5 mM sulfuric acid ( $\text{H}_2\text{SO}_4$ ) as a mobile phase and a Hi-Plex H column (Agilent Technologies, Model No. PL 1170–1830, Santa Clara, CA, USA) with connection to a refractive index detector (RID, Agilent Technologies, Model No. G1362A, Santa Clara, CA, USA) [10,25,27]. The gallic acid, ellagic acid, catechol, and pyrogallol concentrations were quantified using 5 mM sulfuric acid and methanol as a mobile phase with a  $250 \times 4.6$  mm,  $5\ \mu\text{m}$  ZORBAX Eclipse XDB C18 column (Agilent Technologies, Santa Clara, CA, USA), with a diode array detector (DAD, Agilent Technologies, Model No. G1315B, Santa Clara, CA, USA) as adapted from [25,27].

#### 2.5. Model Construction

Mathematical models describing ethanol production under the glucose and xylose ratio of 1:1 [28] and xylitol production from a co-substrate of xylose and glucose at the ratio of 10:1 [29] were modified to describe the cell growth, substrate uptake, and ethanol production from LSW hydrolysate at the glucose and xylose ratio of (2.1–2.2): 1 using *C. tropicalis*. This yeast could uptake and utilize both glucose and xylose for the production of biomass and ethanol [30]. The rate equations for cell growth (Equations (2) and (3)), sugar uptake (Equations (5) and (6)), and ethanol production (Equations (9) and (10)) from glucose and xylose are considered separately as *C. tropicalis* possesses specific transporters for each sugar. The contribution ratio from different sugars to form biomass and ethanol are dissimilar. To quantify such a contribution ratio, the factors of  $\alpha$  for glucose and  $(1 - \alpha)$  for xylose [29] were thus employed as shown in Equations (1), (5), (6) and (8). For the extended cultivation period, during which both glucose and xylose were nearly depleted, the produced ethanol was then considered as an alternative substrate for cell growth, as shown in Equations (4) and (7).

The cell growth rate equation is given as follows:

$$\frac{dx}{dt} = f_x(CF) \times (\alpha r_{x,1} + (1 - \alpha) r_{x,2})x + r_{x,3}x \quad (1)$$

$$r_{x,1} = \mu_{max,1} \times \left( \frac{S_1}{K_{sx,1} + S_1} \right) \left( 1 - \frac{P - P_{ix,1}}{P_{mx,1} - P_{ix,1}} \right) \left( \frac{K_{ix,1}}{K_{ix,1} + S_1} \right) \quad (2)$$

$$r_{x,2} = \begin{cases} \mu_{max,2} \times \left( \frac{S_2}{K_{sx,2} + S_2} \right) \left( 1 - \frac{P - P_{ix,2}}{P_{mx,2} - P_{ix,2}} \right) \left( \frac{K_{ix,2}}{K_{ix,2} + S_2} \right) & , \quad S_2 \geq S_{2,b} \\ 0 & , \quad S_2 < S_{2,b} \end{cases} \quad (3)$$

$$r_{x,3} = \begin{cases} 0 & , \quad S_2 \geq S_{2,a} \\ \mu_{max,3} \times \left( \frac{S_3}{K_{sx,3} + S_3} \right) \left( 1 - \frac{S_3 - P_{ix,3}}{P_{mx,3} - P_{ix,3}} \right) \left( \frac{K_{ix,3}}{K_{ix,3} + S_3} \right) & , \quad S_2 < S_{2,a} \end{cases} \quad (4)$$

The glucose (S1), xylose (S2), and ethanol (S3) uptake rate equations are as follows:

$$\frac{dS_1}{dt} = -CF \times \alpha \times q_{smax,1} \left( \frac{S_1}{K_{ss,1} + S_1} \right) \left( 1 - \frac{P - P_{is,1}}{P_{ms,1} - P_{is,1}} \right) \left( \frac{K_{is,1}}{K_{is,1} + S_1} \right) x \quad (5)$$

$$\frac{dS_2}{dt} = -(1 - \alpha) \times q_{smax,2} \left( \frac{S_2}{K_{ss,2} + S_2} \right) \left( 1 - \frac{P - P_{is,2}}{P_{ms,2} - P_{is,2}} \right) \left( \frac{K_{is,2}}{K_{is,2} + S_2} \right) x \quad (6)$$

$$\frac{dS_3}{dt} = \begin{cases} 0 & , S_2 \geq S_{2,a} \\ -CF \times q_{smax,3} \left( \frac{S_3}{K_{ss,3} + S_3} \right) \left( 1 - \frac{P - P_{is,3}}{P_{ms,3} - P_{is,3}} \right) \left( \frac{K_{is,3}}{K_{is,3} + S_3} \right) x & , S_2 < S_{2,a} \end{cases} \quad (7)$$

The ethanol (P) production rate equation is as follows:

$$\frac{dP}{dt} = f_x(CF) \times (\alpha r_{p,1} + (1 - \alpha) r_{p,2}) x \quad (8)$$

$$r_{p,1} = q_{pmax,1} \left( \frac{S_1}{K_{sp,1} + S_1} \right) \left( 1 - \frac{P - P_{ip,1}}{P_{mp,1} - P_{ip,1}} \right) \left( \frac{K_{ip,1}}{K_{ip,1} + S_1} \right) x \quad (9)$$

$$r_{p,2} = q_{pmax,2} \left( \frac{S_2}{K_{sp,2} + S_2} \right) \left( 1 - \frac{P - P_{ip,2}}{P_{mp,2} - P_{ip,2}} \right) \left( \frac{K_{ip,2}}{K_{ip,2} + S_2} \right) x \quad (10)$$

For this model, the following assumptions were considered: (1) The values of  $K_{sp}$ ,  $P_{ip}$ ,  $P_{mp}$ , and  $K_{ip}$  for the ethanol production rate equation from glucose and xylose are similar to  $K_{ss}$ ,  $P_{is}$ ,  $P_{ms}$ , and  $K_{is}$  for the respective sugar uptake. (2)  $S_{2,a} \geq S_{2,b}$  or the critical xylose concentration initiating the consumption of ethanol for cell growth ( $S_{2,a}$ ) is always higher or equal to the critical xylose concentration causing the cessation of cell growth from xylose ( $S_{2,b}$ ). These terms are governed by the third-order polynomial functions of the  $CF$  in the forms of  $\varepsilon_{III}(CF)^3 + \varepsilon_{II}(CF)^2 + \varepsilon_I(CF) + \varepsilon_0$  and  $\phi_{III}(CF)^3 + \phi_{II}(CF)^2 + \phi_I(CF) + \phi_0$ , respectively. (3) Glucose and xylose are the main substrates for the carbon source and the effects of the by-products are not considered.  $f_x(CF)$  is the third-order polynomial function of the  $CF$  in the form of  $\gamma_{III}(CF)^3 + \gamma_{II}(CF)^2 + \gamma_I(CF) + \gamma_0$ . Two inhibition parameters ( $P_i$  and  $P_m$ ) from ethanol and one non-competitive substrate inhibition parameter ( $K_i$ ) were included. The augmentation of these parameters in modified Monod kinetics rate equations with substrate limitation in an ethanol producing system was elucidated by Leksawasdi et al. [26] for *Zymomonas mobilis* growth and the fermentation of xylose and glucose mixtures. The threshold ethanol concentration ( $P_i$ ) was included to assess the phenomenon by which ethanol would become inhibitory to growth, substrate consumption, and ethanol production when a specific ethanol concentration was reached. In addition, the complete ethanol inhibition was also observed for growth, substrate consumption, and ethanol production when the maximum inhibitory ethanol concentration ( $P_m$ ) was attained, thereby the inclusion of the  $P_m$  term was essential. The simplification of this model was made as stated in assumption (1).

The terms used are declared fully in the Nomenclature section, subscript 1 referring to glucose, subscript 2 referring to xylose, subscript 3 referring to produced ethanol as alternative substrate, and subscript I–III as well as 0 referring to the assigned multiplied coefficients ( $\varepsilon$ ,  $\phi$ ,  $\gamma$ ) to the corresponding numeral exponent of the  $CF$  in third-order polynomial equations.

## 2.6. Parameter Estimation, Optimization, and Estimation of Statistical Parameters

Parameters were estimated using a program written in Microsoft EXCEL with Visual Basic for Applications (VBA) 6.3 [26,28,29] with numerical integration by Euler's method based on least square minimization. The optimal parameters were then determined and assessed for the statistical parameters, including the total residual sum of squares ( $RSS_{total}$ ), total mean square ( $MS_{total}$ ), and correlation coefficient ( $R^2$ ) [29] between the experimental data and the proposed model. Each data point of experimental kinetic data was presented in each graph as an average value with an error bar from the analysis of quintuplicate samples. Statistical differences at the significant level of  $p \leq 0.05$  based on Duncan's



multiple comparisons were assessed using Statistical Packages for the Social Sciences (SPSS, version 17.0) with one-way analyses of variance (ANOVA) [29]. Definitions of the ethanol yield and productivity were provided in a similar manner to previous studies [10,25,29].

### 3. Results and Discussion

#### 3.1. Ethanol Production Kinetics

Twelve batch experiments were assessed using *C. tropicalis* under a batch culture system with total sugar concentrations ranging from 30.6 to 213 g/L at a glucose and xylose ratio of 2:1. The kinetic profiles of glucose and xylose consumption, as well as biomass and ethanol productions, within the total sugar concentration range of 30.6–91.8 g/L are depicted in Figure 1, with the tabulated important kinetic parameters found in Table 1. As shown in Figure 1A,B, glucose and xylose were simultaneously consumed to a certain level within 18 h. However, a slow xylose consumption rate during the first 6 h and incomplete xylose consumption were observed. This might be attributed to the glucose repression [31] in which glucose is the preferred carbon source, where the uptake and/or metabolism of xylose are inhibited by the presence of glucose. After 18 h, *C. tropicalis* began consuming the accumulated ethanol for cell maintenance and the reproduction of the biomass as a decrease in ethanol concentration after attaining the highest peak and an increase in the dried biomass were observed (Figure 1C,D). As a result, the highest ethanol concentration of 25.5 g/L with a yield of 0.30 g/g and productivity of 1.063 g/L/h was achieved at a total sugar concentration of 91.8 g/L using *C. tropicalis*. From Table 1, the highest maximum ( $p \leq 0.05$ ) specific growth rate ( $\mu_{max}$ ) between 0.132 and 0.138 per h was achieved at the CF of 1.6, 1.8, 2.0, and 3.0. The highest maximum ( $p \leq 0.05$ ) specific glucose consumption rate ( $q_{s1,max}$ ) of  $1.294 \pm 0.064$  g/g/h and maximum ( $p \leq 0.05$ ) specific ethanol production rate ( $q_{p,max}$ ) of  $0.755 \pm 0.016$  g/g/h were achieved at a CF of 3.0 and 1.8, respectively. The highest maximum ( $p \leq 0.05$ ) ethanol mass yield ( $Y_{p/s}$ ) of  $0.45 \pm 0.007$  g/g, ethanol productivity ( $Q_p$ ) of  $1.306 \pm 0.021$  g/L/h, and ethanol concentration ( $P_{max}$ ) of  $25.5 \pm 0.58$  g/L were attained at CF of 1.4, 2.0, and 3.0, respectively.

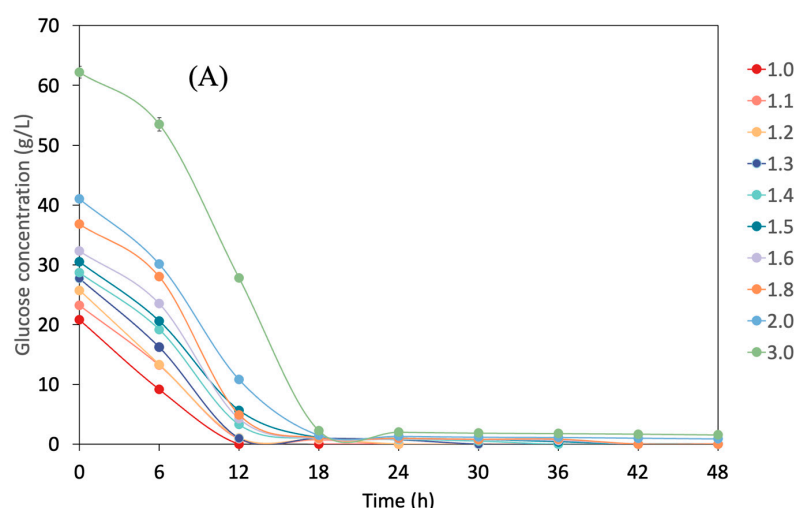
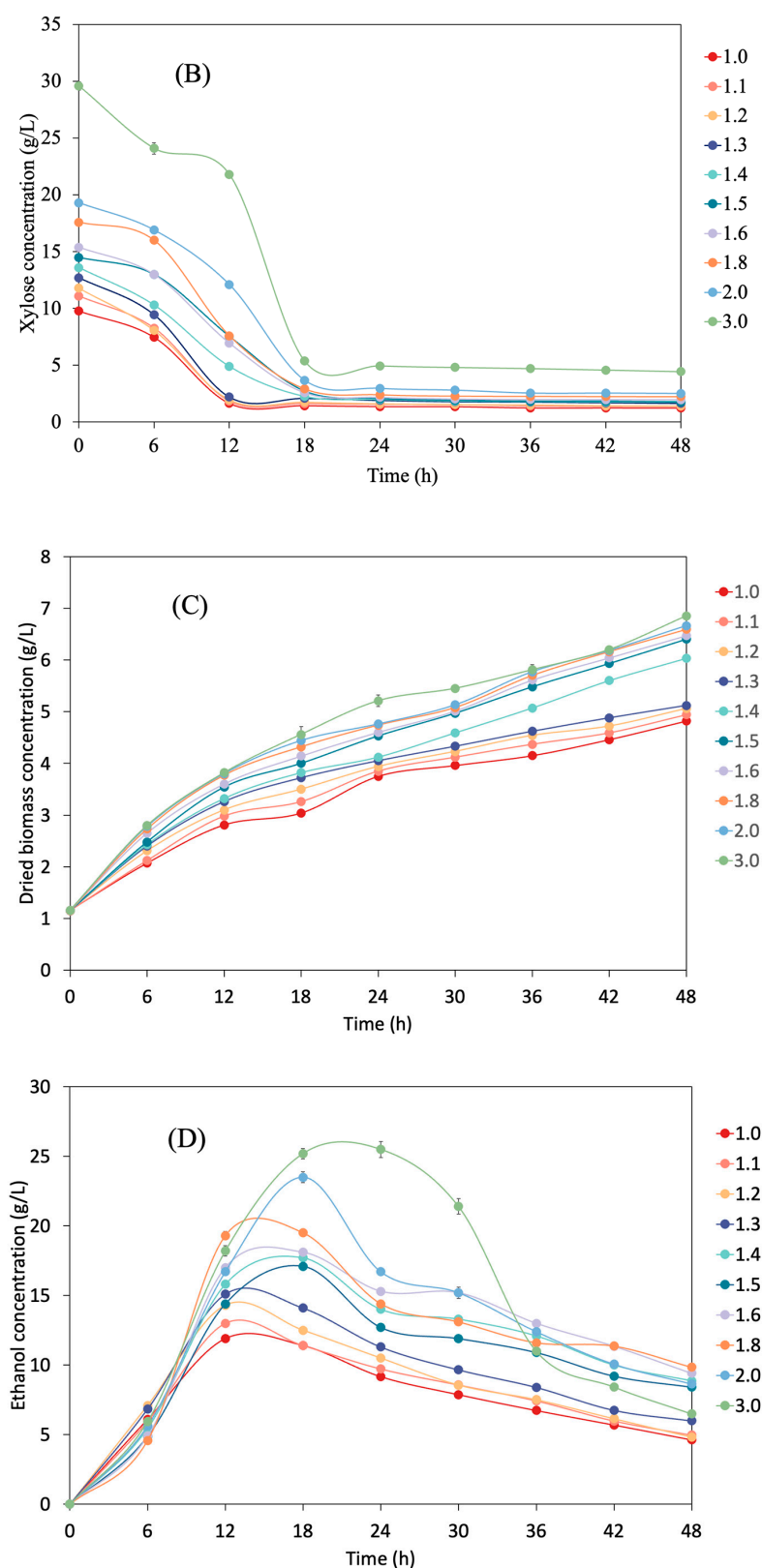


Figure 1. Cont.



**Figure 1.** Kinetics profiles of (A) glucose concentration, (B) xylose concentration, (C) dried biomass concentration, and (D) ethanol concentration by *C. tropicalis* at different substrate concentrations up to 3.0 with a glucose + xylose concentration of 62.2 + 29.6 g/L over 48 h of fermentation. The kinetics profiles for the CF of 5.0 and 7.0 were excluded and are presented separately in Section 3.3 for a clear visual comparison of the profile characteristics at lower substrate concentration ranges. Each data point represents the mean value  $\pm$  standard error (SE) value.

**Table 1.** Analyses of important kinetic parameters including ethanol yield ( $Y_{P/S}$ ) and productivity ( $Q_P$ ) from the experimental kinetic profiles of Figure 1.

CF	S <sub>1</sub> + S <sub>2</sub> (g/L)	$\mu_{max}$ (per h)	$q_{sL,max}$ (g/g/h)	$q_{p,max}$ (g/g/h)	$P_{max}$ (g/L)	$Y_{P/S}$ (g/g)	$Q_P$ (g/L/h)
1.0	20.8 + 9.78	0.094 ± 0.003 <sup>d</sup>	1.202 ± 0.023 <sup>b</sup>	0.630 ± 0.011 <sup>c,d</sup>	11.9 ± 0.26 <sup>j</sup>	0.41 ± 0.009 <sup>b,c</sup>	0.992 ± 0.022 <sup>e,f,g</sup>
1.1	23.2 + 11.1	0.099 ± 0.005 <sup>d</sup>	1.019 ± 0.037 <sup>c,d</sup>	0.607 ± 0.011 <sup>e</sup>	13.0 ± 0.17 <sup>i</sup>	0.41 ± 0.006 <sup>b,c</sup>	1.083 ± 0.014 <sup>d</sup>
1.2	25.7 + 11.8	0.110 ± 0.004 <sup>b,c</sup>	1.191 ± 0.037 <sup>b</sup>	0.682 ± 0.017 <sup>b</sup>	14.3 ± 0.15 <sup>h</sup>	0.41 ± 0.005 <sup>b,c</sup>	1.192 ± 0.013 <sup>c</sup>
1.3	27.7 + 12.7	0.117 ± 0.005 <sup>b</sup>	1.080 ± 0.046 <sup>c</sup>	0.642 ± 0.012 <sup>c</sup>	15.1 ± 0.13 <sup>g</sup>	0.41 ± 0.005 <sup>c</sup>	1.258 ± 0.011 <sup>b</sup>
1.4	28.7 + 13.6	0.119 ± 0.006 <sup>b</sup>	0.922 ± 0.016 <sup>f</sup>	0.600 ± 0.010 <sup>d</sup>	17.7 ± 0.15 <sup>e</sup>	<b>0.45 ± 0.007<sup>a</sup></b>	0.983 ± 0.008 <sup>f</sup>
1.5	30.5 + 14.5	0.122 ± 0.004 <sup>b</sup>	0.909 ± 0.029 <sup>f</sup>	0.528 ± 0.015 <sup>g</sup>	17.1 ± 0.44 <sup>f</sup>	0.42 ± 0.011 <sup>b,c</sup>	0.950 ± 0.024 <sup>g</sup>
1.6	32.3 + 15.4	<b>0.132 ± 0.003<sup>a</sup></b>	1.026 ± 0.012 <sup>c,d</sup>	0.645 ± 0.006 <sup>c</sup>	18.1 ± 0.09 <sup>d</sup>	0.41 ± 0.002 <sup>c</sup>	1.006 ± 0.005 <sup>e</sup>
1.8	36.8 + 17.6	<b>0.136 ± 0.003<sup>a</sup></b>	1.184 ± 0.008 <sup>b</sup>	<b>0.755 ± 0.016<sup>a</sup></b>	19.5 ± 0.05 <sup>c</sup>	0.39 ± 0.002 <sup>d</sup>	1.083 ± 0.003 <sup>d</sup>
2.0	41.0 + 19.3	<b>0.137 ± 0.003<sup>a</sup></b>	0.978 ± 0.023 <sup>e</sup>	0.561 ± 0.007 <sup>f</sup>	23.5 ± 0.38 <sup>b</sup>	0.43 ± 0.009 <sup>b</sup>	<b>1.306 ± 0.021<sup>a</sup></b>
3.0	62.2 + 29.6	<b>0.138 ± 0.006<sup>a</sup></b>	<b>1.294 ± 0.064<sup>a</sup></b>	0.617 ± 0.021 <sup>c,d</sup>	<b>25.5 ± 0.58<sup>a</sup></b>	0.30 ± 0.008 <sup>e</sup>	1.063 ± 0.024 <sup>d</sup>
5.0	104 + 48.5	0.079 ± 0.006 <sup>e</sup>	0.442 ± 0.041 <sup>g</sup>	0.143 ± 0.005 <sup>h</sup>	6.10 ± 0.13 <sup>k</sup>	0.25 ± 0.007 <sup>f</sup>	0.145 ± 0.003 <sup>h</sup>
7.0	145 + 68.0	No observable growth, substrates consumption, product formation					

The values indicate the mean value ± standard error (SE). Different alphabets indicate significant statistical difference ( $p \leq 0.05$ ) among comparison in each column. The bolded and underlined values in each column are the statistical maxima.

In comparison with another yeast used for ethanol production from hydrolysate, in which the maximum ethanol concentration of 46.9 g/L with a yield of 0.43 g/g was achieved from a total sugar concentration of 135 g/L corncob hydrolysate using *C. magnoliae* [32], the highest ethanol concentration of 16.7 g/L was reached at 24 h from longan fruit waste hydrolysate with 180 g/L sugar concentrations using *S. cerevisiae* [33]. The lower ethanol concentration and yield from longan waste hydrolysate as substrate might be attributed to the rich phenolics presented in hydrolysate. Polyphenols, rich in longan seeds and peel, are chemical compounds consisting of two or more phenol structural units [34]. During enzymatic hydrolysis, the hydrolysable tannins were broken down, releasing products such as gallic acid and ellagic acid [35,36]. Meanwhile, the breakdown of polysaccharides may create conditions that facilitate the release of small phenolics such as catechol and pyrogallol.

### 3.2. Effect of Phenolics

In this study, the phenolic concentration levels in LSW enzymatic hydrolysate were ranked in descending order as follows: gallic acid > ellagic acid > pyrogallol > catechol (Figure 2). The growth of *C. tropicalis* was susceptible to gallic and ellagic acids [37]. Although their reactive mechanisms are not fully understood, their presence might result in the disruption of the yeast membrane, preventing the development of cells. The minimum inhibition concentration (MIC) values for the effects of gallic and ellagic acids on *Candida* spp. reported in the literature varied according to the species [38]. The former ranged from 2.5 to 16,000 µg/mL for *C. albicans*, 100 to 4000 µg/mL for *C. parapsilosis*, and *C. krusei*. MIC values for *C. albicans* and *C. tropicalis* were at the highest level of 12,500 µg/mL. The latter ranged from 4 to 1000 µg/mL for all species above [37]. As shown in Figure 2, the highest gallic acid and ellagic acid concentrations in this study were 1006 and 690 mg/L, respectively, which were relatively lower than the abovementioned individual inhibition levels for each phenolic compound. The kinetic of gallic acid in Figure 2 with a CF of 1.0, 1.1, and 1.2 revealed that up to 95% of the initial gallic acid concentration (175 mg/L) decreased after 24 h, while ellagic acid decreased at a relatively lower extent. Thus, the combined effect from the presence of four phenolics, even at a lower concentration, on ethanol production suppression could be evident in the current study. Based on the magnitude difference in the concentration ranges of total sugars (30.6–213 g/L), ethanol (11.4–25.5 g/L), and total phenolic compounds (0.34–1.97 g/L), the inhibitory effect from the phenolic compounds could be eclipsed compared with the total sugars by 90–108-fold and compared with ethanol by 12.9–33.5-fold. Evidently, relatively excellent



model fitting quality was observed, even when the phenolic compounds' inhibitory term was not included (see Section 3.3).

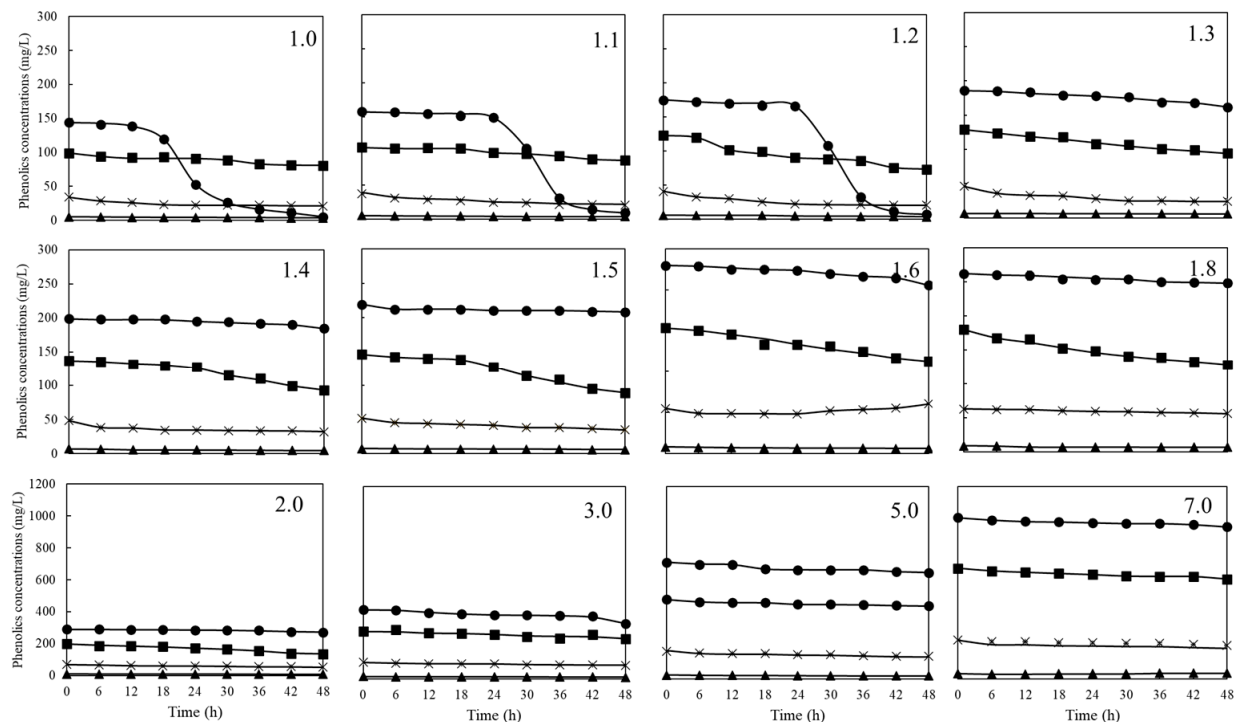


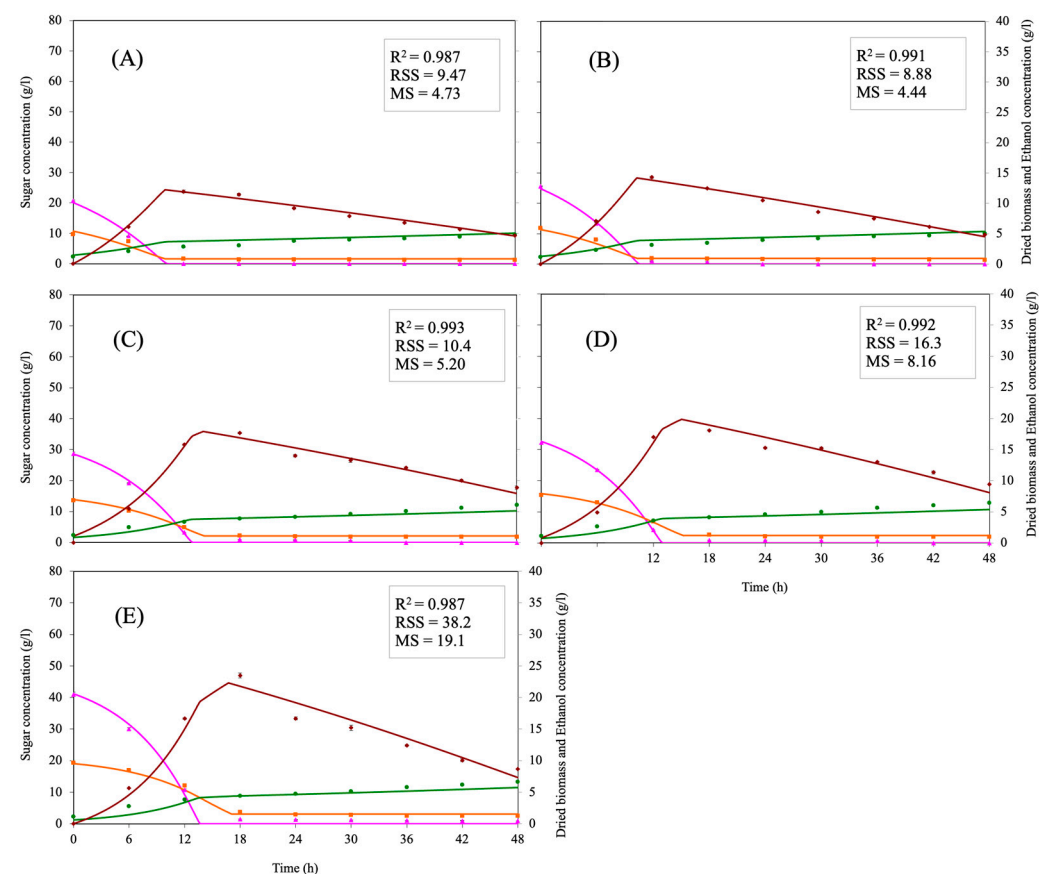
**Figure 2.** Kinetic profiles of gallic acid (solid circle), ellagic acid (solid square), pyrogallol (cross), and catechol (solid triangle) concentrations using *C. tropicalis* at different substrate concentration levels corresponding to concentration factors (CF) of 1.0–7.0. The maxima of y-axis scales in descending rows were 100, 300, and 1200 mg/L, respectively. Each data point represents the mean value  $\pm$  standard error (SE) value. The size of the error bars for all data points were only 0.1–4.0% for a CF of 1.0–1.8 and 0.2–4.0% for a CF of 2.0–7.0, which were well below the visibility range of the employed scales.

### 3.3. Model Validation

Five group experiments using glucose ( $S_1$ ) and xylose ( $S_2$ ) mixture with CF of 1.0, 1.2, 1.4, 1.6, and 2.0 were used for parameters searching. The searched optimal parameters for cell growth, substrate uptake, and ethanol production are shown in Table 2, with the corresponding simulated profiles to the kinetics data shown in Figure 3. The coefficient values in the third-order polynomial equations of  $S_{2,a}$ ,  $S_{2,b}$ , and  $f_x(CF)$  in descending power order from the highest exponent to the lowest exponent were as follows:  $(-0.489, -0.226, 0.0300)$ ,  $(2.68, 1.58, -0.410)$ ,  $(-2.71, -1.74, 1.49)$ , and  $(2.17, 2.08, -0.0896)$ , respectively. Model validation was carried out by comparing the predicted data and additional experimental values with a CF of 1.1, 1.3, 1.5, and 1.8 for interpolation as well as a CF of 3.0 for extrapolation. As shown in Figure 4A–E, cell growth, sugar consumption, and ethanol production were in good agreement between experimental and simulated data with average  $R^2$ ,  $RSS$ , and  $MS$  values of 0.987, 43.0, and 21.5, respectively. Model prediction capability testing was also extended to the CFs of 5.0 and 7.0 (Figure 4F,G) with acceptable agreement. The good agreement between the simulated data from the developed model and experimental data on the fermentation process utilizing LSW hydrolysate within the total sugar concentration range of 30.6–213 g/L under the glucose and xylose ratio of (2.1–2.2): 1 using *C. tropicalis* was thus evident.

**Table 2.** Optimal parameters obtained from the parameter searching process with the RSS minimization strategy.

Equations	Parameters	$S_1$	$S_2$	$S_3$	Units
Cell Growth	$\mu_{max}$	0.0957	0.0472	0.00756	per h
	$K_{sx}$	0.640	3.31	1.35	g/L
	$P_{ix}$	113	45.1	67.2	g/L
	$P_{mx}$	472	136	225	g/L
	$K_{ix}$	517	219	336	g/L
Substrate Uptake	$q_{smax}$	0.865	1.13	0.0548	g/g/h
	$K_{ss}$	0.256	1.65	1.21	g/L
	$P_{is}$	49.6	69.4	10.0	g/L
	$P_{ms}$	153	168	600	g/L
	$K_{is}$	600	175	335	g/L
Ethanol Production	$q_{pmax}$	0.355	0.479	-	g/g/h
	$K_{sp}$	0.256	1.65	-	g/L
	$P_{ip}$	49.6	69.4	-	g/L
	$P_{mp}$	153	168	-	g/L
	$K_{ip}$	600	175	-	g/L

**Figure 3.** Kinetics of the experimental (points) data used in the parameter searching of the proposed model as well as the corresponding simulated fitting (lines) from the model predicting growth of *C. tropicalis* from five concentrations factors (CF) of (A) 1.0, (B) 1.2, (C) 1.4, (D) 1.6, and (E) 2.0. Representations: pink (glucose); orange (xylose); green (dried biomass); and brown (ethanol). Each data point represents the mean value  $\pm$  standard error (SE) value.

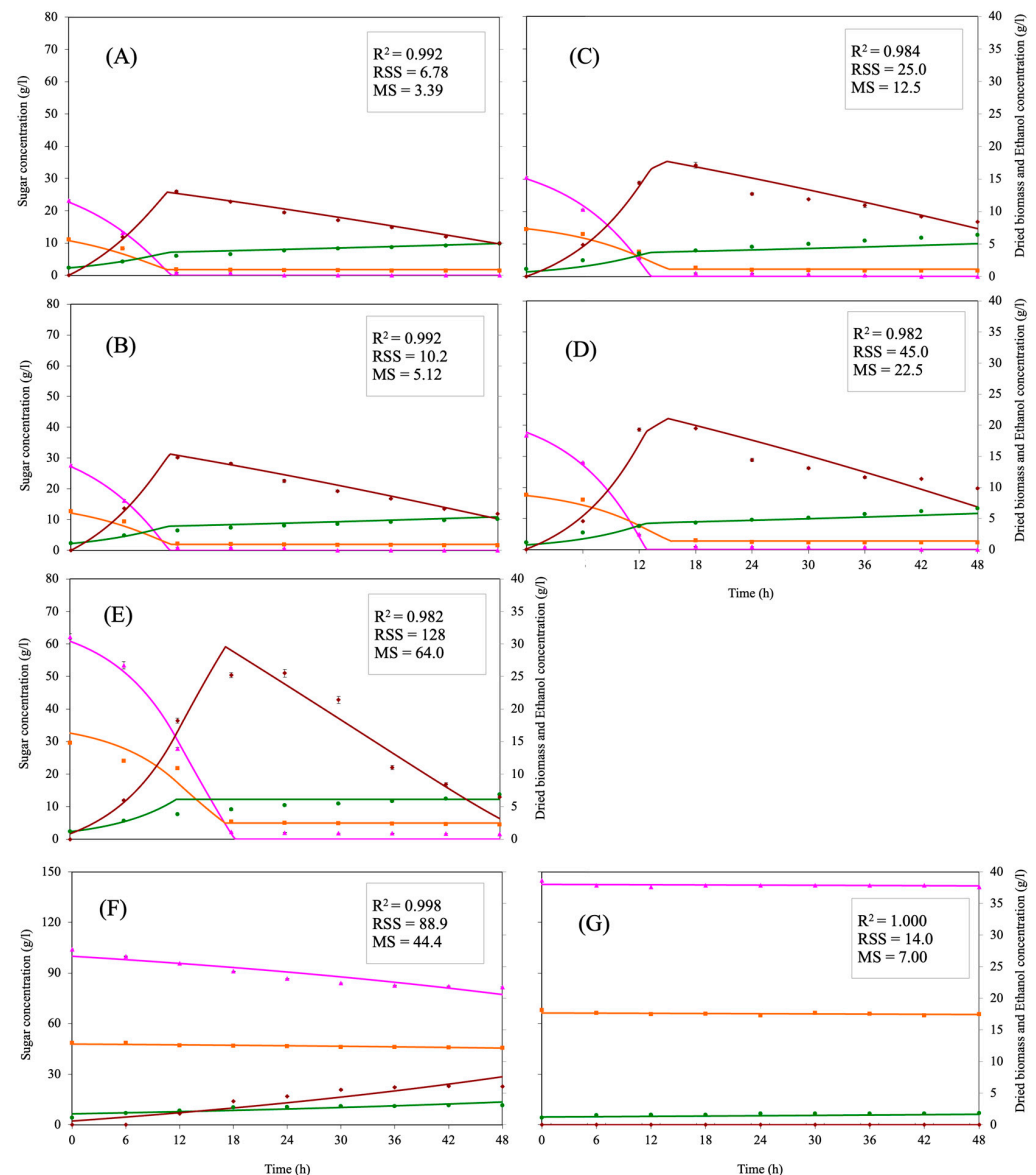


**Figure 4.** Interpolative and extrapolative capabilities of the proposed mathematical model represented by the simulation (lines) and experimental (points) data for kinetics of batch ethanol production by *C. tropicalis* from various concentrations factors (CF). Interpolative capability: (A) 1.1, (B) 1.3, (C) 1.5, and (D) 1.8. Extrapolative capability: (E) 3.0, (F) 5.0, and (G) 7.0. Representations: pink (glucose); orange (xylose); green (dried biomass); and brown (ethanol). The  $R^2$  of 1.000 implied the excellent graph fitting by the model to the experimental data when this number was rounded off to 3 decimal places. Each data point represents the mean value  $\pm$  standard error (SE) value.

### 3.4. Proposed Model

Based on the kinetics of the current fermentation process describing sugar consumption, biomass formation, as well as ethanol production leading to eventual consumption under the assumption of no additional utilized substrate or by-product, a substrate–product switch model was elucidated. This model can be conceptually divided into three key components that influence the rate equations for cell growth ( $dx/dt$ ), substrate uptake ( $ds/dt$ ), and ethanol production ( $dp/dt$ ) with their respective maximum specific values, namely, (1) the effect of glucose, xylose, and ethanol concentration with the incorporation of substrate limitation ( $K_s$ ), substrate inhibition ( $K_i$ ), and product inhibition ( $P_i$  and  $P_m$ ); (2) carbon source allocation between glucose ( $\alpha$ ) and xylose ( $1 - \alpha$ ) to determine the relative contribution of each sugar to cell growth, sugar uptake, and ethanol production; (3) process

effectiveness to capture the impact of substrate availability (reflected by  $CF$ ) and intracellular metabolic efficiency (reflected by growth corrective factor  $f_x(CF)$ ) on fermentation performance. Initially, glucose ( $S_1$ ) and xylose ( $S_2$ ) were consumed as substrates for biomass formation (Equations (2) and (3)) and ethanol production (Equation (8)). However, once sugars were consumed and decreased to certain levels, the produced ethanol switched from being a product ( $P$ ) (Equation (8)) to an alternative substrate (symbol  $P$  switched to  $S_3$ ) (Equation (7)) used to support cell maintenance and a certain level of growth (Equation (4)). In comparison with the Logistic and Monod model describing cell growth, as well as the modified Gompertz, Leudeking–Piret, and Michaelis–Menten model describing ethanol production [39,40], the advantages of the current model are due to the enhanced fermentation efficiency, process predictability, and industrial applicability, facilitated by integrating key biological and kinetic factors into a structured framework of differential rate equations.

### 3.5. Kinetic Characteristics

#### 3.5.1. Substrates and Product Consumptions

The maximum specific growth rate ( $\mu_{max}$ ), maximum specific substrate consumption rate ( $q_{smax}$ ), and maximum specific product formation rate ( $q_{pmax}$ ) are critical parameters in microbial fermentation and bioprocess modeling.  $\mu_{max}$  primarily represents the cellular metabolism for growth with the following descending values of  $\mu_{max,s1} > \mu_{max,s2} > \mu_{max,s3}$ , indicating that the order of substrate preference was therefore glucose, xylose, and ethanol. The contributing factors ( $\alpha$  and  $1 - \alpha$ ) represent the relative preference for sugar utilization, biomass formation, and ethanol production from glucose ( $\alpha$ ) or xylose ( $1 - \alpha$ ). The multiplication of  $\alpha$  and ( $1 - \alpha$ ) with the respective maximum specific values suggests that glucose contributes approximately 2.5 times more to its maximum value than xylose when present in a (2.1–2.2): 1 ratio. The concentration factor ( $CF$ ) is a parameter representing the actual extracellular substrate concentration available for microbial consumption. Additionally,  $f_x(CF)$  is an empirical growth function in the form of a third-order polynomial of the  $CF$  associated with the maximum specific growth rate. It describes how the  $CF$  influences intracellular cell growth and metabolic activity.

#### 3.5.2. Three-Step Metabolism

From the good agreement of the model fitting to experimental data, the three-step metabolism involving extracellular and intracellular activities can be distinctly separated to elucidate a better understanding of the fermentation process (Figure 5). In step I, the  $CF$  was found effective in enhancing glucose uptake but not xylose uptake (Equations (5) and (6)). As a result, the apparent maximum specific glucose consumption rate ( $CF \times \alpha \times q_{smax,1}$ ) increased with a higher sugar concentration, whereas the apparent maximum specific xylose consumption rate ( $(1 - \alpha) \times q_{smax,2}$ ) remained unaffected. This phenomenon might be attributed to glucose repression, where xylose transport is severely inhibited by the presence of glucose [41] despite *C. tropicalis* possessing specific transporters for each sugar. Given that glucose and xylose were initially present in a (2.1–2.2): 1 ratio, *C. tropicalis* could be more sensitive to the availability or effective concentration of glucose than xylose. The glucose uptake rate could be enhanced by increasing the sugar concentration in the medium, whereas the improvement of xylose uptake rate might require targeted strategies to enhance its transport. In step II,  $f_x(CF)$  indicated that glucose and xylose could be effectively converted into ethanol and biomass, and the conversion rates ( $dx/dt$  and  $dp/dt$ ) were improved by higher intracellular sugar concentrations (Equations (1) and (8)). In step III, the produced ethanol was uptaken and utilized as a carbon source to enter the TCA cycle for energy generation or biosynthesis. The  $CF$  in Equation (7) indicates that ethanol uptake was improved with its concentration. However, the  $f_x(CF)$  in the cell growth

equation from ethanol (Equation (4)) indicates that ethanol was inefficient in supporting cell growth. This might be due to the fact ethanol accumulation significantly impacts yeast cells [42]. As a result, step I (sugar uptake) and step III (ethanol consumption) would be crucial steps for control if high ethanol concentration was to be achieved.

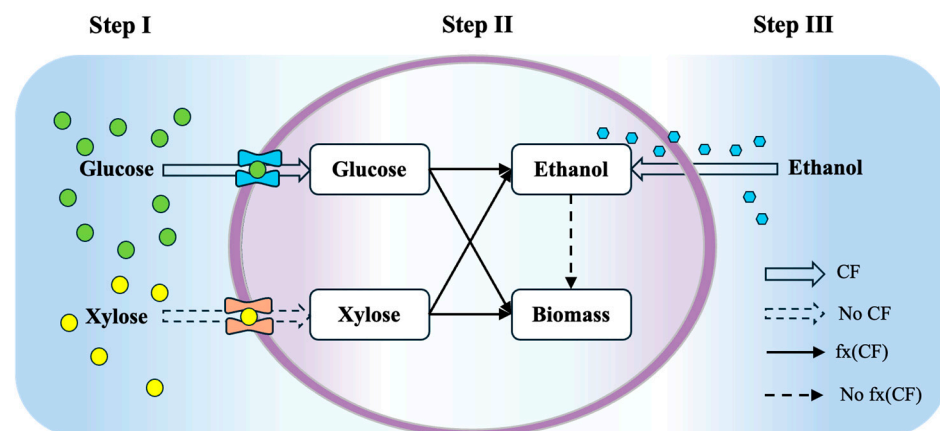


**Figure 5.** Proposed substrate–product switch model. CF—concentration factor applied in the uptake rate equations; No CF—no concentration factor applied;  $f_x(CF)$ —growth corrective factor applied in production equations; and  $f_x(CF)$ —no growth corrective factor applied.

The optimization of the glucose and xylose transporter processes in yeast metabolism are crucial as they are essential rate limiting steps. The enhanced sugar utilization, particularly xylose, and increased *D*-xylonate production by 49.3% in sugarcane bagasse hydrolysate was achieved by modifying the glucose–xylose co-transporter in *C. glycerinogenes* [43]. A similar result in a mixed sugar cultivation utilizing *S. cerevisiae* had been described at which the xylose uptake rate and growth improvement was evident in both substrate systems with the xylose alone and xylose/glucose mixture [44].

### 3.5.3. Correlation Between Xylose Consumption and Ethanol Production

Based on the experimental data analysis, a strong correlation between xylose and ethanol consumption was observed ( $R^2 = 0.982$ ). Two critical xylose concentrations of  $S_{2,a}$  and  $S_{2,b}$  were identified as the key switching points in the rate equations (Equations (3), (4) and (7)).  $S_{2,a}$  represents the critical concentration at which ethanol consumption is triggered, facilitating the transition of ethanol from a product (*P*) to a substrate (*S*<sub>3</sub>) for cell growth.  $S_{2,b}$  is the lowest xylose concentration at which xylose consumption ceases. As shown in Figure 6,  $S_{2,a} \geq S_{2,b}$  indicates that ethanol consumption was initiated at the same time or before xylose was fully depleted. Moreover, a time gap of 0–24 min was observed between the drop from  $S_{2,a}$  to  $S_{2,b}$ . This finding suggests that in fed-batch or continuous systems, new substrate feeding should occur before or at the point of complete sugar depletion. Similarly, in batch systems, ethanol removal should be performed before sugar is fully depleted to optimize production efficiency. One strategy for the optimization of cost-effective ethanol production could be performed by designing a pulse feeding strategy based on the real-time monitoring of both ethanol and evolved CO<sub>2</sub> gas [45,46].

Additionally, the Monod saturation constant or substrate limitation constant ( $K_s$ ) is a parameter representing the substrate concentration at which the maximum specific growth rate of microbe is halved ( $\mu_{max}/2$ ).  $K_s$ , associated with xylose utilization ( $K_{sx,2}$ ), cell growth ( $K_{sx,2}$ ), and ethanol production ( $K_{sp,2}$ ), was relatively higher than glucose, which could indicate the high affinity of the microorganism for glucose. The substrates' inhibitory constants ( $K_i$ ) represented the inhibitory effect of either glucose or xylose on growth ( $K_{ix}$ ), substrate consumption ( $K_{is}$ ), and ethanol production ( $K_{ip}$ ). A higher  $K_i$  value



for glucose indicates that the microorganism exhibits a greater tolerance to a high glucose concentration, meaning that inhibition occurs only at a very high substrate level. During ethanol fermentation, ethanol accumulation significantly impacts yeast cells by disrupting the membrane integrity, resulting in enhanced permeability and a subsequent decrease in cell viability [42]. The current study revealed a maximum ethanol concentration of 25.5 g/L, and the relatively higher values of threshold ethanol concentration ( $P_i$ ) and maximum inhibitory ethanol concentration ( $P_m$ ) in the expression form of  $1 - (P - P_i)/(P_m - P_i)$  would thus result in the net positive effect on cell growth rate ( $dx/dt$ ), sugar uptake ( $ds/dt$ ), and ethanol production ( $dp/dt$ ), especially for xylose uptake and conversion. Similar results were also reported using *S. cerevisiae* [47], where the growth inhibitory effect was absent during the first day of yeast cultivation when ethanol concentration in the cultivation medium was less than 30 g/L. Based on the values of  $P_{ms}$  and  $P_{mp}$  obtained from the model, both cell growth and ethanol production would be completely inhibited when the ethanol concentrations exceeded 153 and 168 g/L, respectively. Moreover, the interaction of low ethanol level on the yeast cells' membrane [48] could increase membrane permeability with potential improvements in the uptake of glucose and xylose.

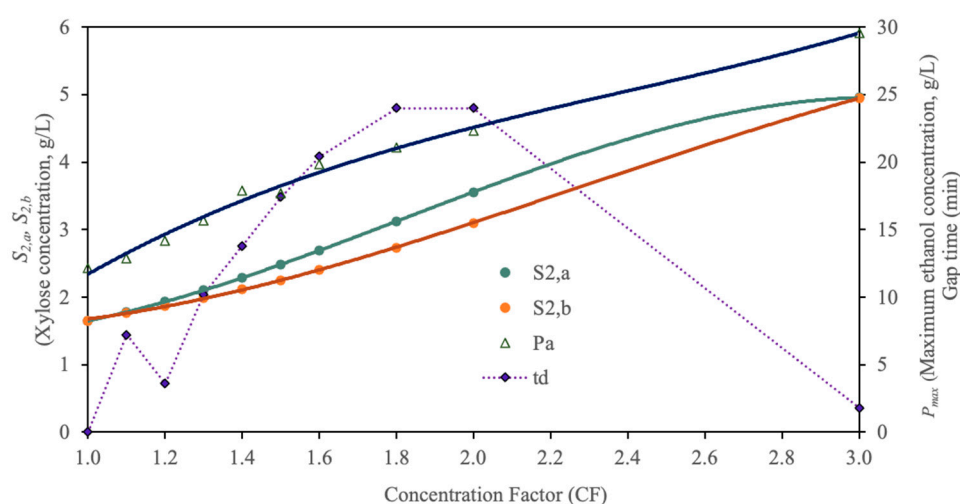


**Figure 6.** Relationships between two critical xylose concentrations to initiate the ethanol uptake step ( $S_{2,a}$ , green line) and cessation of xylose uptake ( $S_{2,b}$ , orange line) with the corresponding maximum ethanol concentration ( $P_{max}$ , blue line) before switching to ethanol consumption mode for each level of concentration factor (CF). The gap duration (purple line) between  $S_{2,a}$  and  $S_{2,b}$  during which ethanol consumption process was initiated and xylose consumption ceased is also shown for each CF.

#### 4. Conclusions

The maximum ethanol concentration of 25.5 g/L with a corresponding ethanol mass yield of 0.30 g/g and productivity of 1.063 g/L/h was achieved from *C. tropicalis* cultivation when the total glucose and xylose concentrations of 91.8 g/L was used as substrates. A new substrate–product switch model was able to describe ethanol production from a mixture of glucose and xylose within concentrations from 30.6 to 213 g/L at a ratio of 2:1. It could accurately simulate the kinetic profiles of cell growth, sugar uptake, and ethanol production with relatively good agreement ( $R^2 = 0.987$ ,  $RSS = 43.0$ ,  $MS = 21.5$ ) between the model and experimental results. A three-step metabolism for ethanol production was characterized by the kinetics of substrate and product consumptions; the ethanol consumption was initiated at the same time or before xylose was fully depleted. These findings provide insights into mixtures of sugar fermentation for ethanol production, with new perspectives for ethanol production improvement based on the developed model.

**Supplementary Materials:** The following supporting information can be downloaded at: <https://www.mdpi.com/article/10.3390/agriculture15141472/s1>, Table S1: Kinetics data of dried biomass, sugars, ethanol, and phenolic compound concentrations for the CF 1.0x of LSW. Table S2: Kinetics data of dried biomass, sugars, ethanol, and phenolic compound concentrations for the CF 1.1x of LSW. Table S3: Kinetics data of dried biomass, sugars, ethanol, and phenolic compound concentrations for the CF 1.2x of LSW. Table S4: Kinetics data of dried biomass, sugars, ethanol, and phenolic compound concentrations for the CF 1.3x of LSW. Table S5: Kinetics data of dried biomass, sugars, ethanol, and phenolic compound concentrations for the CF 1.4x of LSW. Table S6: Kinetics data of dried biomass, sugars, ethanol, and phenolic compound concentrations for the CF 1.5x of LSW. Table S7: Kinetics data of dried biomass, sugars, ethanol, and phenolic compound concentrations for the CF 1.6x of LSW. Table S8: Kinetics data of dried biomass, sugars, ethanol, and phenolic compound concentrations for the CF 1.8x of LSW. Table S9: Kinetics data of dried biomass, sugars, ethanol, and phenolic compound concentrations for the CF 2.0x of LSW. Table S10: Kinetics data of dried biomass, sugars, ethanol, and phenolic compound concentrations for the CF 3.0x of LSW. Table S11: Kinetics data of dried biomass, sugars, ethanol, and phenolic compound concentrations for the CF 5.0x of LSW. Table S12: Kinetics data of dried biomass, sugars, ethanol, and phenolic compound concentrations for the CF 7.0x of LSW.

**Author Contributions:** Conceptualization, J.F. and N.L.; Data curation, J.F., J.K. and N.L.; Formal analysis, J.F., S.L.H., C.T., S.T. and N.L.; Funding acquisition, P.R., S.S. and N.L.; Investigation, J.F.; Methodology, J.F., C.M., K.P., S.S., R.N. and N.L.; Project administration, N.L.; Resources, N.L.; Software, N.L.; Supervision, Y.P., J.K. and N.L.; Validation, J.F., Y.P. and N.L.; Visualization, J.F. and P.R.; Writing—original draft, J.F.; Writing—review and editing, J.F., C.M., S.L.H., C.T., Y.P., P.R., J.K., S.T., K.P., S.S., R.N. and N.L. All authors have read and agreed to the published version of the manuscript.

**Funding:** This research was funded by the National Research Council of Thailand (NRCT) (Grant Number: NRCT5-RSA63004-08), Center of Excellence in Agro-Bio-Circular-Green Industry (Agro-BCG) (Grant Number: CoE67-P001), Office of Research Administration (ORA), Bioprocess Research Cluster (BRC), Faculty of Agro-Industry-Chiang Mai University (CMU). The present study was partially supported by the Thailand Research Fund (TRF) Research Team Promotion Grant, RTA, Senior Research Scholar (Grant Number: N42A671052).

**Institutional Review Board Statement:** Not applicable.

**Informed Consent Statement:** Not applicable.

**Data Availability Statement:** This article's data are available from the corresponding authors upon request.

**Acknowledgments:** The authors would like to thank funding support from the National Research Council of Thailand (NRCT) (Grant Number: NRCT5-RSA63004-08), Center of Excellence in Agro-Bio-Circular-Green Industry (Agro-BCG) (Grant Number: CoE67-P001), Office of Research Administration (ORA), Bioprocess Research Cluster (BRC), Faculty of Agro-Industry-Chiang Mai University (CMU). The present study was partially supported by the Thailand Research Fund (TRF) Research Team Promotion Grant, RTA, Senior Research Scholar (Grant Number: N42A671052). TISTR is also thanked for the microbial strain support.

**Conflicts of Interest:** The authors declare no conflicts of interest.

## Abbreviations

$\alpha$	Contributing factors for glucose (no unit)
$\varepsilon$	Coefficient value for the third-order polynomial equation of $S_{2,a}$
$\varphi$	Coefficient value for the third-order polynomial equation of $S_{2,b}$
$\gamma$	Coefficient value for the third-order polynomial equation of $f_x(CF)$
$\mu_{max}$	Maximum specific growth rate (per h)
CF	Concentration factor (no unit)

$f_x(CF)$	Growth corrective factor—a third polynomial function of the $CF$ (no unit)
$K_i$	Substrate inhibition constant associated with a specific rate equation (g/L)
$K_{ip}$	$K_i$ for ethanol production rate equation (g/L)
$K_{is}$	$K_i$ for substrate utilization rate equation (g/L)
$K_{ix}$	$K_i$ for growth rate equation (g/L)
$K_s$	Substrate limitation constant associated with a specific rate equation (g/L)
$K_{sp}$	$K_s$ for ethanol production rate equation (g/L)
$K_{ss}$	$K_s$ for substrate utilization rate equation (g/L)
$K_{sx}$	$K_s$ for growth rate equation (g/L)
$MS$	Mean square (no unit)
$P$	Ethanol concentration (g/L)
$P_i$	Threshold ethanol concentration causing inhibition for a specific rate equation (g/L)
$P_{ip}$	$P_i$ for ethanol production rate equation (g/L)
$P_{is}$	$P_i$ for substrate utilization rate equation (g/L)
$P_{ix}$	$P_i$ for growth rate equation (g/L)
$P_m$	Maximum inhibitory ethanol concentration for a specific rate equation (g/L)
$P_{max}$	Maximum ethanol concentration in each cultivation condition (g/L)
$P_{mp}$	$P_m$ for ethanol production rate equation (g/L)
$P_{ms}$	$P_m$ for substrate utilization rate equation (g/L)
$P_{mx}$	$P_m$ for growth rate equation (g/L)
$Q_P$	Ethanol productivity (g/L/h)
$q_{s,max}$	Maximum specific substrate utilization rate (g/g/h)
$q_{p,max}$	Maximum specific ethanol production rate (g/g/h)
$R^2$	Correlation coefficient (no unit)
$RSS$	Residual sum of squares (g/L) <sup>2</sup>
$S_1$	Glucose concentration (g/L)
$S_2$	Xylose concentration (g/L)
$S_{2,a}$	Critical xylose concentration initiating the consumption of ethanol for cell growth (g/L)
$S_{2,b}$	Critical xylose concentration causing the cessation of cell growth from xylose (g/L)
$S_3$	Ethanol concentration as an alternative substrate (g/L)
$x$	Biomass concentration (g/L)
$Y_{P/S}$	Mass yield of produced ethanol over the consumed xylose and glucose (g/g)

## References

- Green, Y. The Application of Ethanol Fuel: Taking the United States as An Example. *Biol. Evid.* **2024**, *14*, 1–9. [\[CrossRef\]](#)
- Feng, J.; Techapun, C.; Phimolsiripol, Y.; Phongthai, S.; Khemacheewakul, J.; Taesuwan, S.; Mahakuntha, C.; Porninta, K.; Htike, S.L.; Kumar, A. Utilization of agricultural wastes for co-production of xylitol, ethanol, and phenylacetylcarbinol: A review. *Bioresour. Technol.* **2023**, *392*, 129926. [\[CrossRef\]](#)
- Rajeswari, S.; Baskaran, D.; Saravanan, P.; Rajasimman, M.; Rajamohan, N.; Vasseghian, Y. Production of ethanol from biomass—Recent research, scientometric review and future perspectives. *Fuel* **2022**, *317*, 123448. [\[CrossRef\]](#)
- Maduzzi, J.; Thomas, H.Y.; Fidelis, J.D.; de Carvalho, J.V.; Silva, E.C.; da Costa Filho, J.D.; Cavalcante, J.D.; dos Santos, E.S.; de Santana Souza, D.F.; de Araújo Padilha, C.E. Ethanol Production from Corn cob Assisted by Polyethylene Glycol and Conversion of Lignin-Rich Residue into Lignosulfonate and Phenolic Acids. *BioEnergy Res.* **2024**, *17*, 1598–1611. [\[CrossRef\]](#)
- Vennila, T.; Karuna, M.S.; Srivastava, B.K.; Venugopal, J.; Surakasi, R. New Strategies in Treatment and Enzymatic Processes: Ethanol Production From Sugarcane Bagasse. In *Human Agro-Energy Optimization for Business and Industry*; IGI Global: Hershey, PA, USA, 2023; pp. 219–240. [\[CrossRef\]](#)
- Taghizadeh-Alisaraei, A.; Tatari, A.; Khanali, M.; Keshavarzi, M. Potential of biofuels production from wheat straw biomass, current achievements and perspectives: A review. *Biofuels* **2023**, *14*, 79–92. [\[CrossRef\]](#)
- Kumar, A.; Jain, S.; Kumar, S. Bio-oil production from rice Straw: Evaluating solvent effects and two-stage liquefaction process. *Biomass Bioenergy* **2025**, *200*, 107980. [\[CrossRef\]](#)
- Tian, B.; Wang, S.; Wang, J.; Feng, F.; Xu, L.; Ma, X.; Tian, Y. A comprehensive evaluation on thermo-chemical potential of longan waste for the production of chemicals and carbon materials. *Fuel* **2023**, *334*, 126655. [\[CrossRef\]](#)
- Nguyen, T.V.T.; Unpaprom, Y.; Ramaraj, R. Enhanced fermentable sugar production from low grade and damaged longan fruits using cellulase with algal enzymes for bioethanol production. *Emergent Life Sci. Res.* **2020**, *6*, 26–31. [\[CrossRef\]](#)

10. Wattanapanom, S.; Muenseema, J.; Techapun, C.; Jantanasakulwong, K.; Sanguanchaipaiwong, V.; Chaityaso, T.; Hanmoungjai, P.; Seesuriyachan, P.; Khemacheewakul, J.; Nunta, R. Kinetic parameters of *Candida tropicalis* TISTR 5306 for ethanol production process using an optimal enzymatic digestion strategy of assorted grade longan solid waste powder. *Chiang Mai J. Sci* **2019**, *46*, 1036–1054.
11. Kumar, S.; Agarwal, G.; Sreekrishnan, T. Optimization of co-culture condition with respect to aeration and glucose to xylose ratio for bioethanol production. *Indian Chem. Eng.* **2023**, *65*, 233–248. [\[CrossRef\]](#)
12. Nosrati-Ghods, N.; Harrison, S.T.; Isafiade, A.J.; Tai, S.L. Ethanol from biomass hydrolysates by efficient fermentation of glucose and xylose—A review. *ChemBioEng Rev.* **2018**, *5*, 294–311. [\[CrossRef\]](#)
13. Farias, D.; Maugeri-Filho, F. Sequential fed batch extractive fermentation for enhanced bioethanol production using recycled *Spathaspora passalidarum* and mixed sugar composition. *Fuel* **2021**, *288*, 119673. [\[CrossRef\]](#)
14. Ochoa-Chacón, A.; Martinez, A.; Poggi-Varaldo, H.M.; Villa-Tanaca, L.; Ramos-Valdivia, A.C.; Ponce-Noyola, T. Xylose metabolism in bioethanol production: *Saccharomyces cerevisiae* vs. non-*Saccharomyces* yeasts. *BioEnergy Res.* **2022**, *15*, 905–923. [\[CrossRef\]](#)
15. da Silva, D.D.V.; Machado, E.; Danelussi, O.; dos Santos, M.G.; da Silva, S.S.; Dussán, K.J. Repeated-batch fermentation of sugarcane bagasse hemicellulosic hydrolysate to ethanol using two xylose-fermenting yeasts. *Biomass Convers. Biorefinery* **2022**, *12*, 4321–4331. [\[CrossRef\]](#)
16. Gao, J.; Yu, W.; Li, Y.; Jin, M.; Yao, L.; Zhou, Y.J. Engineering co-utilization of glucose and xylose for chemical overproduction from lignocellulose. *Nat. Chem. Biol.* **2023**, *19*, 1524–1531. [\[CrossRef\]](#)
17. Germec, M.; Turhan, I. Ethanol production from acid-pretreated and detoxified tea processing waste and its modeling. *Fuel* **2018**, *231*, 101–109. [\[CrossRef\]](#)
18. Alvarado-Santos, E.; Aguilar-López, R.; Neria-González, M.I.; Romero-Cortés, T.; Robles-Olvera, V.J.; López-Pérez, P.A. A novel kinetic model for a cocoa waste fermentation to ethanol reaction and its experimental validation. *Prep. Biochem. Biotechnol.* **2023**, *53*, 167–182. [\[CrossRef\]](#)
19. Germec, M.; Karhan, M.; Demirci, A.; Turhan, I. Kinetic modeling, sensitivity analysis, and techno-economic feasibility of ethanol fermentation from non-sterile carob extract-based media in *Saccharomyces cerevisiae* biofilm reactor under a repeated-batch fermentation process. *Fuel* **2022**, *324*, 124729. [\[CrossRef\]](#)
20. Asiedu, N.Y.; Bamaalabong, P.P.; Johnson, J.E.; Bonsu, J.K.; Addo, A. Modeling, simulations, and Simulink developments in the analysis of optimal control of temperature and pH in a batch ethanol fermentation process. *J. Eng. Appl. Sci.* **2024**, *71*, 195. [\[CrossRef\]](#)
21. da Silva Fernandes, F.; de Souza, É.S.; Carneiro, L.M.; Alves Silva, J.P.; de Souza, J.V.B.; da Silva Batista, J. Current ethanol production requirements for the yeast *Saccharomyces cerevisiae*. *Int. J. Microbiol.* **2022**, *2022*, 7878830. [\[CrossRef\]](#)
22. Todhanakasem, T.; Wu, B.; Simeon, S. Perspectives and new directions for bioprocess optimization using *Zymomonas mobilis* in the ethanol production. *World J. Microbiol. Biotechnol.* **2020**, *36*, 112. [\[CrossRef\]](#)
23. Mann, S.; Sharma, J.G.; Kataria, R. Optimization of acidic pre-treatment conditions using response surface methodology for ethanol production from *Pistia stratiotes* using *Saccharomyces cerevisiae* and *Pichia stipitis*. *Biomass Convers. Biorefinery* **2025**, *15*, 4333–4348. [\[CrossRef\]](#)
24. Jeyaram, K.; Murugan, D.; Velmurugan, S.; Prabhu, A.A.; Raja, S.; Bose, S.A.; Balakrishnan, D. Investigation of the influence of *Candida tropicalis* on bioethanol production using sugarcane bagasse: Stochastic and in silico analysis. *Environ. Sci. Pollut. Res.* **2024**, *31*, 64476–64492. [\[CrossRef\]](#)
25. Porninta, K.; Khemacheewakul, J.; Techapun, C.; Phimolsiripol, Y.; Jantanasakulwong, K.; Sommanee, S.; Mahakuntha, C.; Feng, J.; Htike, S.L.; Moukamnerd, C. Pretreatment and enzymatic hydrolysis optimization of lignocellulosic biomass for ethanol, xylitol, and phenylacetylcarbinol co-production using *Candida magnoliae*. *Front. Bioeng. Biotechnol.* **2024**, *11*, 1332185. [\[CrossRef\]](#)
26. Nunta, R.; Techapun, C.; Kuntiya, A.; Hanmuangjai, P.; Moukamnerd, C.; Khemacheewakul, J.; Sommanee, S.; Reungsang, A.; Boonmee Kongkeitkajorn, M.; Leksawasdi, N. Ethanol and phenylacetylcarbinol production processes of *Candida tropicalis* TISTR 5306 and *Saccharomyces cerevisiae* TISTR 5606 in fresh juices from longan fruit of various sizes. *J. Food Process. Preserv.* **2018**, *42*, e13815. [\[CrossRef\]](#)
27. Dhanani, T.; Shah, S.; Kumar, S. A validated high-performance liquid chromatography method for determination of tannin-related marker constituents gallic acid, corilagin, chebulagic acid, ellagic acid and chebulinic acid in four *Terminalia* species from India. *J. Chromatogr. Sci.* **2015**, *53*, 625–632. [\[CrossRef\]](#)
28. Leksawasdi, N.; Joachimsthal, E.L.; Rogers, P.L. Mathematical modelling of ethanol production from glucose/xylose mixtures by recombinant *Zymomonas mobilis*. *Biotechnol. Lett.* **2001**, *23*, 1087–1093. [\[CrossRef\]](#)
29. Feng, J.; Techapun, C.; Phimolsiripol, Y.; Rachtanapun, P.; Phongthai, S.; Khemacheewakul, J.; Taesuwan, S.; Porninta, K.; Htike, S.L.; Mahakuntha, C. Co-substrate model development and validation on pure sugars and corncob hemicellulosic hydrolysate for xylitol production. *Sci. Rep.* **2024**, *14*, 25928. [\[CrossRef\]](#)

30. Queiroz, S.d.S.; Jofre, F.M.; Bianchini, I.d.A.; Boaes, T.d.S.; Bordini, F.W.; Chandel, A.K.; Felipe, M.d.G.d.A. Current advances in *Candida tropicalis*: Yeast overview and biotechnological applications. *Biotechnol. Appl. Biochem.* **2023**, *70*, 2069–2087. [\[CrossRef\]](#)
31. Leksawasdi, N.; Breuer, M.; Hauer, B.; Rosche, B.; Rogers, P.L. Kinetics of pyruvate decarboxylase deactivation by benzaldehyde. *Biocatal. Biotransformation* **2003**, *21*, 315–320. [\[CrossRef\]](#)
32. Martínez-Jimenez, F.; Pereira, I.; Ribeiro, M.; Sargo, C.; dos Santos, A.; Zanella, E.; Stambuk, B.; Ienczak, J.; Morais, E.; Costa, A. Integration of first-and second-generation ethanol production: Evaluation of a mathematical model to describe sucrose and xylose co-fermentation by recombinant *Saccharomyces cerevisiae*. *Renew. Energy* **2022**, *192*, 326–339. [\[CrossRef\]](#)
33. Nguyen, T.V.T.; Unpaprom, Y.; Manmai, N.; Whangchai, K.; Ramaraj, R. Impact and significance of pretreatment on the fermentable sugar production from low-grade longan fruit wastes for bioethanol production. *Biomass Convers. Biorefinery* **2022**, *12*, 1605–1617. [\[CrossRef\]](#)
34. Zhang, X.; Li, Z.; Yang, P.; Duan, G.; Liu, X.; Gu, Z.; Li, Y. Polyphenol scaffolds in tissue engineering. *Mater. Horiz.* **2021**, *8*, 145–167. [\[CrossRef\]](#)
35. Singh, B.; Singh, J.P.; Kaur, A.; Singh, N. Insights into the phenolic compounds present in jambolan (*Syzygium cumini*) along with their health-promoting effects. *Int. J. Food Sci. Technol.* **2018**, *53*, 2431–2447. [\[CrossRef\]](#)
36. Mohammed, Y. Isolation and characterization of tannic acid hydrolysing bacteria from soil. *Biochem. Anal. Biochem.* **2016**, *5*, 254. [\[CrossRef\]](#)
37. Teodoro, G.R.; Brighenti, F.L.; Delbem, A.C.B.; Delbem, Á.C.B.; Khouri, S.; Gontijo, A.V.L.; Pascoal, A.C.; Salvador, M.J.; Koga-Ito, C.Y. Antifungal activity of extracts and isolated compounds from *Buchenavia tomentosa* on *Candida albicans* and non-*albicans*. *Future Microbiol.* **2015**, *10*, 917–927. [\[CrossRef\]](#)
38. Salih, E.Y.; Julkunen-Tiitto, R.; Luukkanen, O.; Fyhrqvist, P. Anti-*Candida* activity of extracts containing ellagitannins, triterpenes and flavonoids of *Terminalia brownii*, a medicinal plant growing in semi-arid and Savannah woodland in Sudan. *Pharmaceutics* **2022**, *14*, 2469. [\[CrossRef\]](#)
39. Dodić, J.M.; Vučurović, D.G.; Dodić, S.N.; Grahovac, J.A.; Popov, S.D.; Nedeljković, N.M. Kinetic modelling of batch ethanol production from sugar beet raw juice. *Appl. Energy* **2012**, *99*, 192–197. [\[CrossRef\]](#)
40. Agu, K.C.; Oduola, M.K. Kinetic modeling of ethanol production by batch fermentation of sugarcane juice using immobilized yeast. *Glob. J. Eng. Technol. Adv* **2021**, *7*, 124–136. [\[CrossRef\]](#)
41. Rages, A.A.; Haider, M.M.; Aydin, M. Alkaline hydrolysis of olive fruits wastes for the production of single cell protein by *Candida lipolytica*. *Biocatal. Agric. Biotechnol.* **2021**, *33*, 101999. [\[CrossRef\]](#)
42. Aiello, E.; Arena, M.P.; De Vero, L.; Montanini, C.; Bianchi, M.; Mescola, A.; Alessandrini, A.; Pulvirenti, A.; Gullo, M. Wine Yeast Strains Under Ethanol-Induced Stress: Morphological and Physiological Responses. *Fermentation* **2024**, *10*, 631. [\[CrossRef\]](#)
43. Qiao, Y.; Li, C.; Lu, X.; Zong, H.; Zhuge, B. Transporter engineering promotes the co-utilization of glucose and xylose by *Candida glycerinogenes* for D-xylonate production. *Biochem. Eng. J.* **2021**, *175*, 108150. [\[CrossRef\]](#)
44. Reider Apel, A.; Ouellet, M.; Szmidt-Middleton, H.; Keasling, J.D.; Mukhopadhyay, A. Evolved hexose transporter enhances xylose uptake and glucose/xylose co-utilization in *Saccharomyces cerevisiae*. *Sci. Rep.* **2016**, *6*, 19512. [\[CrossRef\]](#)
45. Hung, Y.-H.R.; Chae, M.; Sauvageau, D.; Bressler, D.C. Adapted feeding strategies in fed-batch fermentation improve sugar delivery and ethanol productivity. *Bioengineered* **2023**, *14*, 2250950. [\[CrossRef\]](#)
46. Sandri, J.P.; Ramos, M.D.; Perez, C.L.; Mesquita, T.J.; Zangirolami, T.C.; Milessi, T.S. Bioreactor and process design for 2G ethanol production from xylose using industrial *S. cerevisiae* and commercial xylose isomerase. *Biochem. Eng. J.* **2023**, *191*, 108777. [\[CrossRef\]](#)
47. Zhang, Q.; Wu, D.; Lin, Y.; Wang, X.; Kong, H.; Tanaka, S. Substrate and product inhibition on yeast performance in ethanol fermentation. *Energy Fuels* **2015**, *29*, 1019–1027. [\[CrossRef\]](#)
48. Auesukaree, C. Molecular mechanisms of the yeast adaptive response and tolerance to stresses encountered during ethanol fermentation. *J. Biosci. Bioeng.* **2017**, *124*, 133–142. [\[CrossRef\]](#)

**Disclaimer/Publisher’s Note:** The statements, opinions and data contained in all publications are solely those of the individual author(s) and contributor(s) and not of MDPI and/or the editor(s). MDPI and/or the editor(s) disclaim responsibility for any injury to people or property resulting from any ideas, methods, instructions or products referred to in the content.